A New Torque Control Method for Torque Ripple Minimization of BLDC Motors With Un-Ideal Back EMF

Article *in* IEEE Transactions on Power Electronics · April 2008

DOI: 10.1109/TPEL.2007.915667 · Source: IEEE Xplore

3 authors, including:

Haifeng Lu
Tsinghua University
14 PUBLICATIONS **276** CITATIONS

SEE PROFILE

A New Torque Control Method for Torque Ripple Minimization of BLDC Motors With Un-Ideal Back EMF

Haifeng Lu, Lei Zhang, and Wenlong Qu

***Abstract*—In classical control of brushless dc (BLDC) motors, flux distribution is assumed trapezoidal and fed current is controlled rectangular to obtain a desired constant torque. However, in reality, this assumption may not always be correct, due to nonuniformity of magnetic material and design trade-offs. These factors, together with current controller limitation, can lead to an undesirable torque ripple. This paper proposes a new torque control method to attenuate torque ripple of BLDC motors with un-ideal back electromotive force (EMF) waveforms. In this method, the action time of pulses, which are used to control the corresponding switches, are calculated in the torque controller regarding actual back EMF waveforms in both normal conduction period and commutation period. Moreover, the influence of finite dc bus supply voltage is considered in the commutation period. Simulation and experimental results are shown that, compared with conventional rectangular current control, the proposed torque control method results in apparent reduction of the torque ripple.**

***Index Terms*—Brushless dc (BLDC) motors, electromotive force (EMF), torque ripple.**

I. Introduction

PERMANENT magnet brushless dc (BLDC) motors are now widely used in many applications, such as servo drives, computer peripheral equipments, and electric vehicles due to their high power density, high efficiency and easier control. An idealized brushless dc motor has a trapezoidal back electromotive force (EMF) waveform. For this back EMF waveform it can be shown that zero torque ripple is produced when the motor is fed by a rectangular current waveform [1]. However, for practical reasons, nonuniformity of magnetic material and design trade-offs make it hard to produce the desired trapezoidal back EMF waveform exactly. Therefore, torque ripple appears even though rectangular current is fed in conventional control. Moreover, since the motor windings are inductive, the current controller has often no ability to produce the required di/dt in the commutation period owing to finite dc bus supply voltage, the resulting torque ripple is called commutation torque ripple.

Manuscript received April 17, 2007; revised August 6, 2007. Recommended for publication by Associate Editor F. Z. Peng.

H. F. Lu and W. L. Qu are with the State Key Lab of Power Systems, Department of Electrical Engineering, Tsinghua University, Beijing 100084, China (e-mail: lhf01@mails.tsinghua.edu.cn; qwl@mail.tsinghua.edu.cn).

L. Zhang is with Santak Electronics, Ltd. Co., Guangdong 518101, China (e-mail: lei-zhang02@mails.tsinghua.edu.cn).

Digital Object Identifier 10.1109/TPEL.2007.915667

A great deal of study has been devoted to reducing these torque ripples of the BLDC motor with un-ideal back EMF waveforms. The interaction between the back EMF and the current excitation has been analyzed [2]–[5]. Le-Huy *et al.* [2] recognized that torque ripple could be reduced by selecting appropriate current harmonics. In [3], the torque ripples were analyzed using the exponential Fourier series and the current harmonics were determined in closed form. In [4] Favre *et al.* obtained predetermined current harmonics to eliminate both mutual and cogging torque ripple components. Hanselman *et al.* [5] extended the prior works to include the case of finite dc bus supply voltage. However, these works assume that all three phases have identical back EMF waveforms, and the back EMF waveform and motor excitation current exhibit half-wave symmetry. Park *et al.* [6], [7] proposed a new approach to optimize current waveform based on $d-q$ frame, which results in minimum torque ripple and maximum efficiency of BLDC motor drives. An instantaneous torque control method was presented in [8]–[10]. Low *et al.* [8] designed an instantaneous torque control algorithm based on a variable structure strategy [9] in $d-q$ frame, and the instantaneous torque feedback signal is obtained using least squares parameter estimator [10]. In [11] Colamartino *et al.* introduced a torque estimation method. However, the estimated torque must be filtered to remove the noise produced in the calculation of current derivatives, and the estimator can't be used at low speed due to voltage drop in resistances and freewheeling diodes. Kang *et al.* [12] presented a torque control method in which the required phase terminal voltage is calculated from the torque controller in the two-phase conducting period and in the commutation period. However, the finite dc bus supply voltage, which results in finite ability of torque controller, is neglected. French *et al.* [13] introduced a generalized algorithm, which calculates the optimized current reference by estimating the torque from the rate of change of co-energy with respect to rotor position, to reduce torque ripple. Liu *et al.* [14] described the application of direct torque control (DTC) to BLDC motor drives to achieve instantaneous torque control and reduced torque ripple. In this method, a sliding-mode observer is employed to estimate the un-ideal back EMF waveform, and a simplified extended Kalman filter is used to estimate the rotor speed. Both are combined to estimate instantaneous torque [15]. In [16] Carlson *et al.* analyzed commutation torque ripple theoretically. Furthermore, commutation torque ripple compensation technique had been dealt with by a number of authors [17]–[20]. For instance, one of these compensation techniques is based on the strategy that the current slopes of the

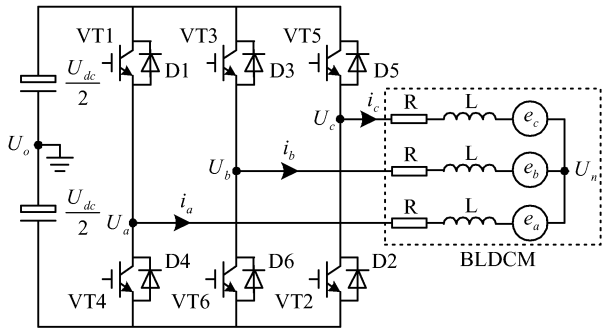

Fig. 1. Configuration of BLDC motor fed with VSI.

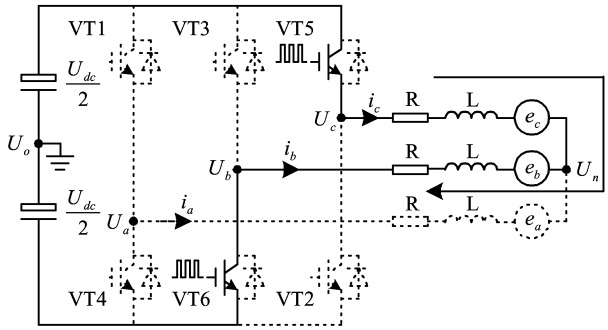

Fig. 2. Normal conduction period.

incoming and the outgoing phases in the commutation period should be equalized, whereas both the analysis and the compensation technique neglect the influence of un-ideal back EMF waveforms.

This paper proposes a new torque control method for minimizing the torque ripple of the BLDC motor with un-ideal back EMF waveforms. The BLDC motor operates in the two-phase conduction mode. The duty cycle of the corresponding switches is pre-calculated in the torque controller regarding the actual back EMF waveforms in both normal conduction period and commutation period. In addition, the finite dc bus supply voltage and resulting finite capability of torque controller are considered in the commutation period. Simulation and experimental results are presented which compared with that in the conventional rectangular current control, it shows that the method proposed is effective in reducing the torque ripple.

II. Proposed Torque Control Method

A BLDC motor is fed by a conventional three-phase voltage source inverter, and its configuration is shown in Fig. 1, where R, L, e, U, i, U_n, and U_o represent the armature resistance, inductance, back EMF, terminal voltage, phase current, motor neutral voltage, and inverter neutral voltage, respectively. The torque equation of a brushless dc motor can be expressed as follows:

$$T_e = \frac{e_a i_a + e_b i_b + e_c i_c}{\omega_m} \tag{1}$$

where ω_m is the motor speed.

In the two-phase conduction mode, there are six combinations of the stator excitation in one cycle. Each combination lasts for 60° electrical degrees, which is called normal conduction period. In order to produce maximum torque, the inverter commutation should be performed every 60° electrical degrees, which is called commutation period. In this period, all three phases conduct because the commutation requires a finite time due to the phase inductance.

A. Normal Conduction Period

In the normal conduction period, only two phases conduct. Assuming at a particular step, phase C and phase B are conducting where current flows into phase C and then out phase B. Referring to Fig. 2, it shows switches VT5 and VT6 are chopping. The phase voltage equations in the normal conduction period can be written as (2) by introducing the switching function S

$$\begin{cases} S \cdot \frac{U_{\rm dc}}{2} = i_c R + L\frac{di_c}{dt} + e_c + U_{\rm no} \\ -S \cdot \frac{U_{\rm dc}}{2} = i_b R + L\frac{di_b}{dt} + e_b + U_{\rm no} \end{cases} \tag{2}$$

where $S = 1$ denotes switching on and $S = -1$ denotes switching off.

At the time when $i_c = -i_b$, the voltage difference between neutrals of the motor and inverter can be described as

$$U_{\rm no} = -\frac{(e_c + e_b)}{2}. \tag{3}$$

It is assumed that the motor armature resistance is relatively small and its affect is neglected. The current derivative of phase C is given by

$$\frac{di_c}{dt} = \begin{cases} \frac{U_{\rm dc}}{2L} + \frac{e_b - e_c}{2L}, & \text{at } S = 1 \\ -\frac{U_{\rm dc}}{2L} + \frac{e_b - e_c}{2L}, & \text{at } S = -1 \end{cases}. \tag{4}$$

From (4), it can be seen that the slope of the current is related with the switching function S. Assuming the duty cycle of switches VT5 and VT6 is D_n, the sampling period of the torque controller is T_s. So S maintains 1 during $D_n T_s$ and -1 during $(1 - D_n)T_s$. Equation (4) can be arranged as (5) using the state-space averaging technique mentioned in literature [19]

$$\left\langle \frac{di_c}{dt} \right\rangle_{\rm Ts} = \frac{U_{\rm dc}(2D_n - 1)}{2L} + \frac{e_b - e_c}{2L} \tag{5}$$

where "$\langle\rangle_{\rm Ts}$" denotes average value in the period of T_s. Assuming that e_c and e_b maintain constant during sampling period, after a sampling period, the current of phase C can be obtained from (5) as follows:

$$i_{c(k+1)} = \frac{U_{dc(k)}[2D_{n(k)} - 1]T_s}{2L} + \frac{[e_{b(k)} - e_{c(k)}]T_s}{2L} + i_{c(k)} \tag{6}$$

where $i_{c(k)}$ is the initial value of i_c in (k) th sampling period.

Current of phase B can be obtained from (7) with the same deducing process

$$i_{b(k+1)} = \frac{U_{dc(k)}[1 - 2D_{n(k)}]T_s}{2L} + \frac{[e_{c(k)} - e_{b(k)}]T_s}{2L} + i_{b(k)}. \tag{7}$$

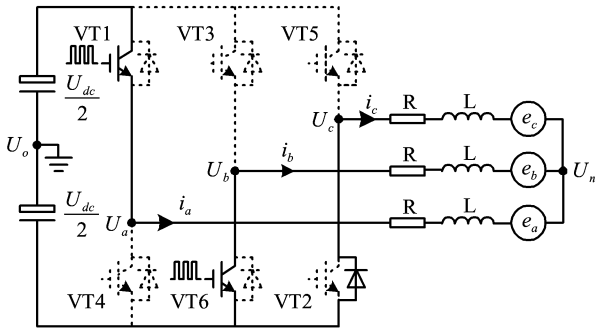

Fig. 3. Commutation between VT1 and VT5.

Combining (6) and (7), the torque equation can be expressed as

$$T_{e(k+1)} = T_{e(k)} + \frac{U_{dc(k)} T_s [2D_{n(k)} - 1][e_{c(k)} - e_{b(k)}]}{2\omega_{m(k)} L} - \frac{[e_{c(k)} - e_{b(k)}]^2 T_s}{2\omega_{m(k)} L} \quad (8)$$

where $T_{e(k)} = (i_{b(k)} e_{b(k)} + i_{c(k)} e_{c(k)})/\omega_{m(k)}$ is feedback torque from last sampling period. For a given torque reference $T_{\rm ref}$, if $T_{e(k+1)} = T_{\rm ref}$, then the duty cycle $D_{n(k)}$, which is used to control switches VT5 and VT6, can be solved as

$$D_{n(k)} = \frac{[T_{\rm ref} - T_{e(k)}]\omega_{m(k)} L}{U_{dc(k)}[e_{c(k)} - e_{b(k)}] T_s} + \frac{e_{c(k)} - e_{b(k)}}{2U_{dc(k)}} + \frac{1}{2}. \quad (9)$$

Equation (9) shows that the duty cycle $D_{n(k)}$ can be calculated with some variables, such as dc supply voltage, feedback torque and actual back EMF waveform. The objective of the calculated duty cycle is to make torque feedback follow the torque reference to reduce torque ripple in normal conduction period.

B. Commutation Period

The inverter commutation occurred every 60° electrical degrees to produce maximum torque. All three phases conduct in the commutation period due to the armature inductance. Assuming at a particular commutation process, the current transfer from phase C to phase A is considered. This transfer is performed by switching off VT5 and switching on VT1. During the transfer, current i_a called incoming phase current increases through VT1, current i_c called outgoing phase current decreases gradually through the anti-parallel diode D2, and current i_b called un-commutated phase current is not involved in the commutation. Referring to Fig. 3, switches VT1 and VT6 are chopping, diode D2 is freewheeling.

Three phase voltage equations in the commutation period can be written as

$$\begin{cases} S \cdot \frac{U_{\rm dc}}{2} = R i_a + L\frac{di_a}{dt} + e_a + U_{\rm no} \\ -S \cdot \frac{U_{\rm dc}}{2} = R i_b + L\frac{di_b}{dt} + e_b + U_{\rm no} \\ -\frac{U_{\rm dc}}{2} = R i_c + L\frac{di_c}{dt} + e_c + U_{\rm no} \end{cases}. \quad (10)$$

The voltage difference between the motor neutral and the inverter neutral can be expressed as

$$U_{\rm no} = -\frac{U_{\rm dc}}{6} - \frac{e_a + e_b + e_c}{3}. \quad (11)$$

According to the switching function S, the current slope of phase A is described as

$$\frac{di_a}{dt} = \begin{cases} \frac{2U_{\rm dc}}{3L} + \frac{e_b + e_c - 2e_a}{3L}, & \text{at } S = 1 \\ -\frac{U_{\rm dc}}{3L} + \frac{e_b + e_c - 2e_a}{3L}, & \text{at } S = -1 \end{cases}. \quad (12)$$

Assuming the duty cycle of switches VT1 and VT6 is D_c. In the commutation period, S maintains 1 during $D_c T_s$ and -1 during $(1 - D_c)T_s$. The average current slope of phase A can be arranged as

$$\left\langle \frac{di_a}{dt} \right\rangle_{\rm Ts} = \frac{U_{\rm dc}(3D_c - 1)}{3L} + \frac{e_b + e_c - 2e_a}{3L}. \quad (13)$$

Solving the differential (13), the current of phase A can be obtained as:

$$i_{a(k+1)} = \frac{T_s}{3L}\left[U_{dc(k)}(3D_{c(k)} - 1) + e_{b(k)} + e_{c(k)} - 2e_{a(k)}\right] + i_{a(k)} \quad (14)$$

The currents of phase B and C can be obtained with same deducing process (15), shown at the bottom of the page.

Combining (14) and (15), the torque equation can be expressed as

$$T_{e(k+1)} = \frac{U_{dc(k)} T_s}{3\omega_{m(k)} L} \times \left[3D_{c(k)}\left(e_{a(k)} - e_{b(k)}\right) + 2e_{b(k)} - e_{a(k)} - e_{c(k)}\right] - \frac{g\left(e_{a(k)}, e_{b(k)}, e_{c(k)}\right) T_s}{3\omega_{m(k)} L} + T_{e(k)} \quad (16)$$

where $T_{e(k)} = (i_{a(k)} e_{a(k)} + i_{b(k)} e_{b(k)} + i_{c(k)} e_{c(k)})/\omega_{m(k)}$ is the feedback torque from last sampling period, and $g(e_{a(k)}, e_{b(k)}, e_{c(k)}) = (e_{a(k)} - e_{b(k)})^2 + (e_{b(k)} - e_{c(k)})^2 + (e_{c(k)} - e_{a(k)})^2$. If $T_{e(k+1)} = T_{\rm ref}$, the duty cycle $D_{c(k)}$, which is used to control switches VT1 and VT6, can be solved as

$$D_{c(k)} = \frac{\left[T_{\rm ref} - T_{e(k)}\right]\omega_{m(k)} L}{U_{dc(k)}\left[e_{a(k)} - e_{b(k)}\right] T_s} - \frac{2e_{b(k)} - e_{a(k)} - e_{c(k)}}{3\left[e_{a(k)} - e_{b(k)}\right]} + \frac{g\left(e_{a(k)}, e_{b(k)}, e_{c(k)}\right)}{3U_{dc(k)}\left[e_{a(k)} - e_{b(k)}\right]}. \quad (17)$$

$$\begin{cases} i_{b(k+1)} = \frac{T_s}{3L}\left[U_{dc(k)}\left(2 - 3D_{c(k)}\right) + e_{a(k)} + e_{c(k)} - 2e_{b(k)}\right] + i_{b(k)} \\ i_{c(k+1)} = -\frac{U_{dc(k)} T_s}{3L} + \frac{\left[e_{a(k)} + e_{b(k)} - 2e_{c(k)}\right] T_s}{3L} + i_{c(k)} \end{cases} \quad (15)$$

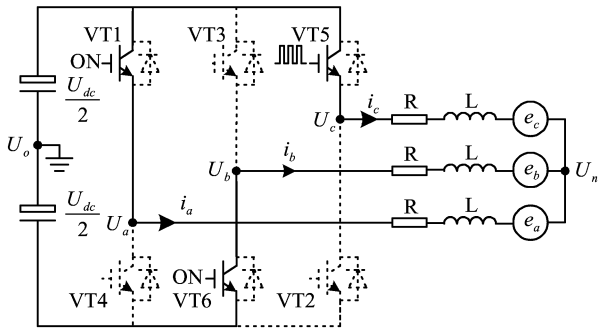

Fig. 4. Commutation period considering finite dc bus supply voltage.

It shows that torque feedback can follow torque reference by means of the calculated duty cycle $D_{c(k)}$ in the commutation period. However, in reality, even though the calculated duty cycle $D_{c(k)}$ reaches 100%, the slope of the incoming phase current i_a maybe slower due to the finite dc bus supply voltage. Because the slope of the outgoing phase current i_c is fast, therefore, a current dip produces in the un-commutated phase current i_b, this results in a commutation torque ripple.

C. Considering Finite DC Bus Supply Voltage

If the calculated duty cycle $D_{c(k)}$ reaches 100%, but the torque feedback still can't follow the torque reference, the slope of the outgoing phase current i_c can be slowed down by switching on VT5 to compensate the current dip in the un-commutated phase current i_b, as well as the commutation torque ripple. Referring to Fig. 4, switches VT1 and VT6 are ON state, VT5 is chopping.

Three phase voltage equations in the commutation period can be written as

$$\begin{cases} \frac{U_{\rm dc}}{2} = Ri_a + L\frac{di_a}{dt} + e_a + U_{\rm no} \\ -\frac{U_{\rm dc}}{2} = Ri_b + L\frac{di_b}{dt} + e_b + U_{\rm no} \\ S\cdot\frac{U_{\rm dc}}{2} = Ri_c + L\frac{di_c}{dt} + e_c + U_{\rm no} \end{cases}. \tag{18}$$

The voltage difference between the motor neutral and the inverter neutral is

$$U_{\rm no} = S\cdot\frac{U_{\rm dc}}{6} - \frac{e_a+e_b+e_c}{3}. \tag{19}$$

With the switching function S, the current slope of phase A can be expressed as

$$\frac{di_a}{dt} = \begin{cases} \frac{U_{\rm dc}}{3L} + \frac{e_b+e_c-2e_a}{3L}, & {\rm at}\, S=1 \\ \frac{2U_{\rm dc}}{3L} + \frac{e_b+e_c-2e_a}{3L}, & {\rm at}\, S=-1 \end{cases}. \tag{20}$$

Assuming the duty cycle of VT5 is D_o, the switching function S maintains 1 during D_oT_s and -1 during $(1-D_o)T_s$. The average slope of phase A current can be obtained as

$$\left\langle \frac{di_a}{dt} \right\rangle_{T_s} = \frac{U_{\rm dc}(2-D_o)}{3L} + \frac{e_b+e_c-2e_a}{3L}. \tag{21}$$

Three phase current equations can be arranged as (22), shown at the bottom of the page.

So, the torque equation can be calculated as

$$\begin{aligned} T_{e(k+1)} = {} & \frac{U_{dc(k)}T_s}{3\omega_{m(k)}L} \\ & \times \left[D_{o(k)}\left(2e_{c(k)} - e_{a(k)} - e_{b(k)}\right)\right. \\ & \left. + 2e_{a(k)} - e_{b(k)} - e_{c(k)}\right] \\ & - \frac{g\left(e_{a(k)}, e_{b(k)}, e_{c(k)}\right)T_s}{3\omega_{m(k)}L} + T_{e(k)}. \end{aligned} \tag{23}$$

If $T_{e(k+1)} = T_{\rm ref}$, the duty cycle $D_{o(k)}$, which is used to control VT5, can be determined as

$$\begin{aligned} D_{o(k)} = {} & \frac{3\left[T_{\rm ref} - T_{e(k)}\right]\omega_{m(k)}L}{U_{dc(k)}\left[2e_{c(k)} - e_{a(k)} - e_{b(k)}\right]T_s} \\ & - \frac{2e_{a(k)} - e_{b(k)} - e_{c(k)}}{2e_{c(k)} - e_{b(k)} - e_{a(k)}} \\ & + \frac{g\left(e_{a(k\}}, e_{b(k)}, e_{c(k)}\right)}{U_{dc(k)}\left[2e_{c(k)} - e_{a(k)} - e_{b(k)}\right]}. \end{aligned} \tag{24}$$

The duty cycle D_o is used to slow down the slope of the outgoing phase current i_c, so as to reduce the current dip existed in the un-commutated phase i_b in the commutation period, and to compensate the commutation torque ripple caused by finite dc supply voltage. When the outgoing phase current is reduced to zero, the regulation of D_o can be stopped.

III. Simulation and Experiment Results

To verify the feasibility of the proposed method, simulations and experiments are carried out. Fig. 5 shows the control system schematic of the brushless dc motor. A surface-mounted three-phase brushless dc motor, which has an un-ideal back EMF waveform, is dealt with in this paper. The parameters of the motor are shown in the Appendix.

In Fig. 5, two current sensors are used to sample currents of phase A and C, and one voltage sensor to sample dc bus supply voltage. Three Hall sensors, from which the motor speed ω_m and the rotor position θ are calculated out, are placed in the brushless dc motor to produce phase commutation signals. The control board is built based on a DSP TMS320F240. The required duty cycle is calculated in torque controller. Commuta-

$$\begin{cases} i_{a(k+1)} = \frac{T_s}{3L}\left[e_{b(k)} + e_{c(k)} - 2e_{a(k)} + U_{dc(k)}\left(2 - D_{o(k)}\right)\right] + i_{a(k)} \\ i_{b(k+1)} = \frac{T_s}{3L}\left[e_{a(k)} + e_{c(k)} - 2e_{b(k)} - U_{dc(k)}\left(1 + D_{o(k)}\right)\right] + i_{b(k)} \\ i_{c(k+1)} = \frac{T_s}{3L}\left[e_{a(k)} + e_{b(k)} - 2e_{c(k)} + U_{dc(k)}\left(2D_{o(k)} - 1\right)\right] + i_{c(k)} \end{cases} \tag{22}$$

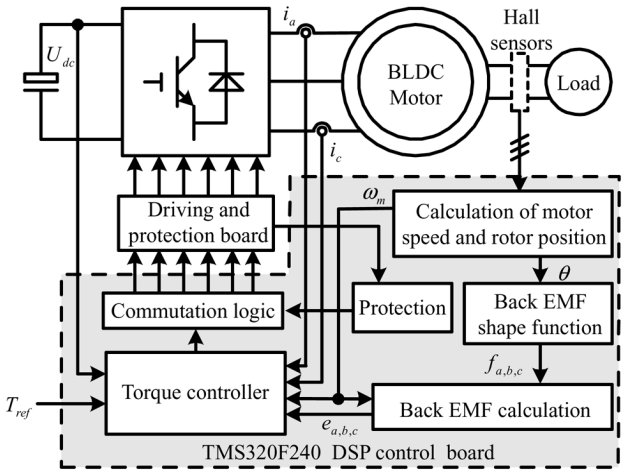

Fig. 5. Function diagram of BLDC motor control system.

tion logic is implemented in DSP and gate drive signals are sent to six IGBT switches through a driving and protection board. Besides, a DAC board based on DAC7624 is designed to output variables such as torque, actual back EMF and rotor position.

A. Observation of Back EMF

Assuming the back EMF of brushless dc motors is proportional to the motor speed [14]. Thus the EMF can be calculated from rotor speed using shape functions f_a, f_b and f_c, as described in (25)

$$\begin{cases} e_a = f_a(\theta) \cdot \omega_m \\ e_b = f_b(\theta) \cdot \omega_m \\ e_c = f_c(\theta) \cdot \omega_m \end{cases} . \tag{25}$$

The actual back EMF waveforms can be measured by the constant speed test for the brushless dc motor. Thus the back EMF with regard to position (or angle) can be obtained, as shown in Fig. 6. In fact, for any position, the value of back EMF is relevant to the speed. Take phase C for example, the relationship between the value of EMF and the motor speed is shown in Fig. 7, where six curves represent six different positions in the EMF waveform. From Figs. 6 and 7, it can be seen that the actual waveforms are significantly distorted comparing to the ideal 120° plat trapezoidal back EMF. In Fig. 7, the value of back EMF is proportion to the speed for given position, which verified above assumption.

The rotor position and rotor speed can be obtained through three Hall sensors. Using shape functions, which are stored in DSP, the estimated back EMF can be calculated on-line by (25).

Fig. 8 shows the calculated rotor position θ and the signal of Hall sensor. From this figure, rotor position changes from 0° to 60° for three times uniformly between two pulse-edges of sensor signal, whose distance is 180° electrical degrees. Then the back EMF plat waveforms of conducting phases can be obtained by table look-up and linear interpolation using shape functions f_a, f_b and f_c, as shown in Fig. 9. These two figures indicate that calculating of estimated back EMF and rotor position works well.

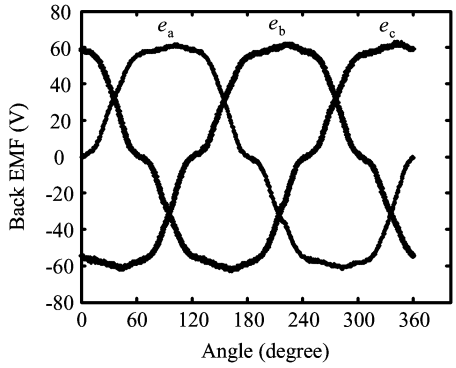

Fig. 6. Measured back EMF waveforms at 1300r/min.

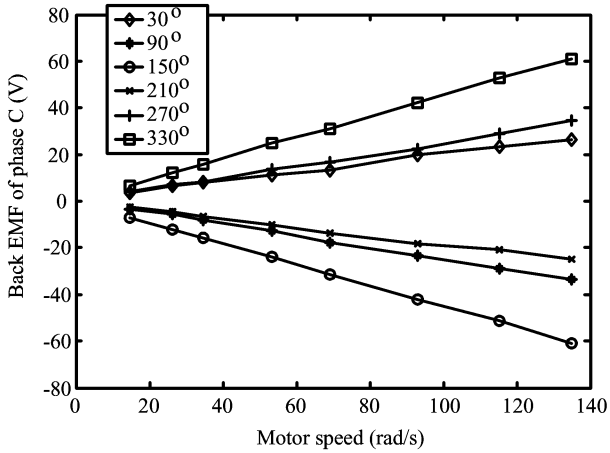

Fig. 7. Back EMF of phase C with the motor speed.

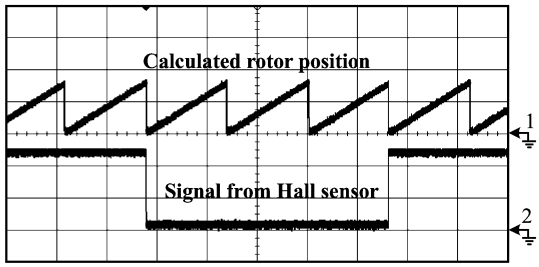

Fig. 8. Calculating of rotor position (rotor position: 35^o/div, sensor signal: 2 V/div, time: 5 ms/div).

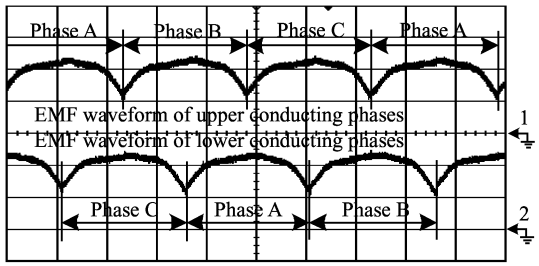

Fig. 9. Estimated Back EMF using shape function (8.2 V/div, 5 ms/div).

B. Simulation Results

With conventional current control, the BLDC motor is fed by ideal 120° rectangular current. However, the torque waveform

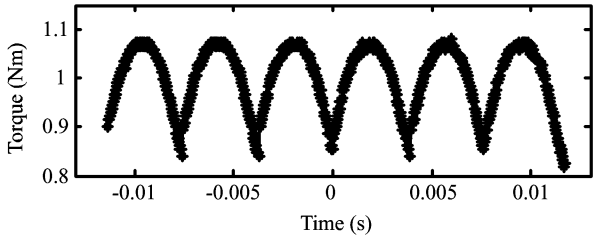

Fig. 10. Torque ripple with conventional current control.

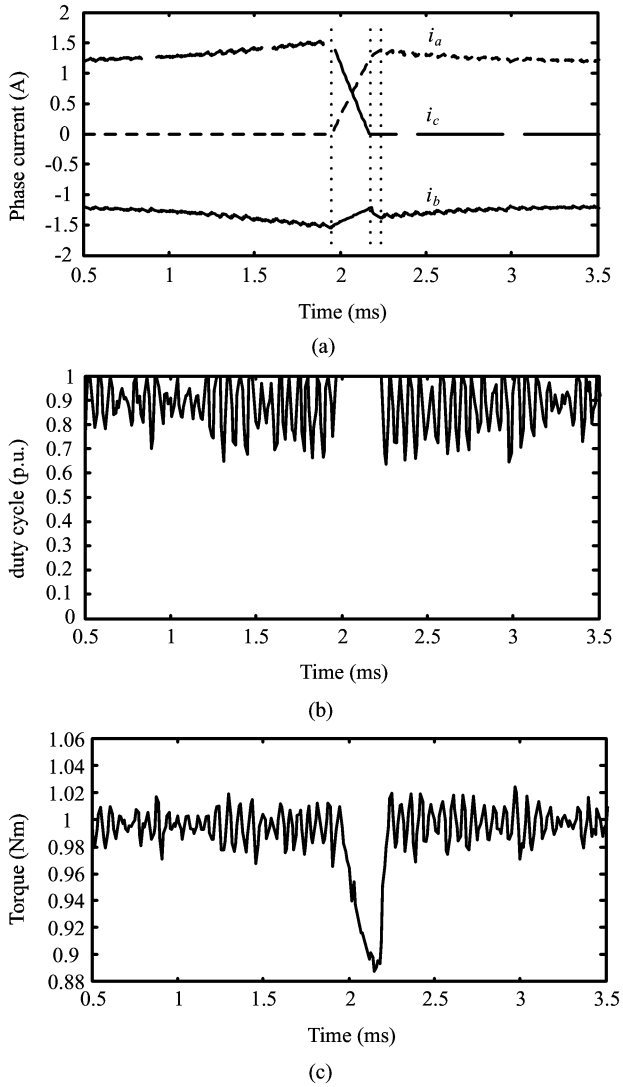

Fig. 11. Torque control neglecting finite dc bus supply voltage. (a) Three phase currents. (b) Calculated duty cycle. (c) Torque waveform.

is distorted seriously as shown in Fig. 10, because of un-ideal back EMF waveform.

Fig. 11 shows the simulation results of torque control neglecting finite dc bus supply voltage. VT5 and VT6 chop before commutation, and VT6 and VT1 chop after commutation. The duty cycle of PWM signal is D_n. In the commutation period, VT5 is switched off and VT1 is switched on. The outgoing phase current i_c decreases through the anti-parallel diode D2 and the incoming phase current i_a increases through VT1. The duty cycle of PWM signal, which is used to control VT6

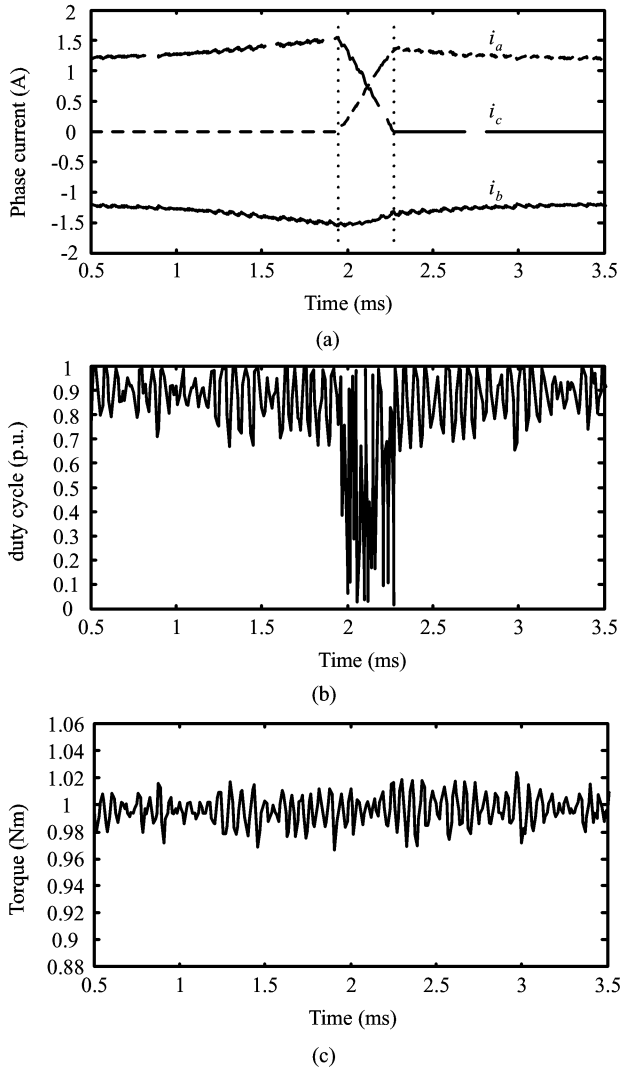

Fig. 12. Torque control considering finite dc bus supply voltage. (a) Three phase currents. (b) Calculated duty cycle. (c) Torque waveform.

and VT1, is D_c. In Fig. 11(a), the descending speed of i_c is larger than the raising speed of i_a, so a current dip occurs in the un-commutated phase current i_b. Fig. 11(b) shows the calculated duty cycle D_n and D_c in the normal conduction period and the commutation period, respectively. Fig. 11(c) shows the resulting torque waveform. It can be seen that torque ripple in the normal conduction period has been reduced with the calculated D_n. However, the commutation torque ripple exists even though the calculated D_c reaches 100% in the commutation period.

Fig. 12 shows the simulation results of torque control considering finite dc bus supply voltage. In Fig. 12(a), the current dip existing in the un-commutated phase i_b has been reduced by slowing down the slope of the outgoing phase current i_c. Fig. 12(b) shows the calculated D_n used in the normal conduction period, and D_o used in the commutation period. In this period, VT6 and VT1 are ON state, and VT5, which should be switched off at the beginning of commutation, is controlled with D_o. Fig. 12(c) shows the resulting torque waveform. It can be seen that torque ripples in both the normal conduction period and the commutation period have been reduced.

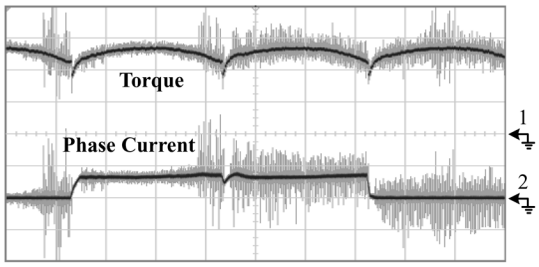

Fig. 13. Torque and phase current with conventional rectangular control (torque: 2.54 Nm/div, current: 10 A/div, time: 2 ms/div).

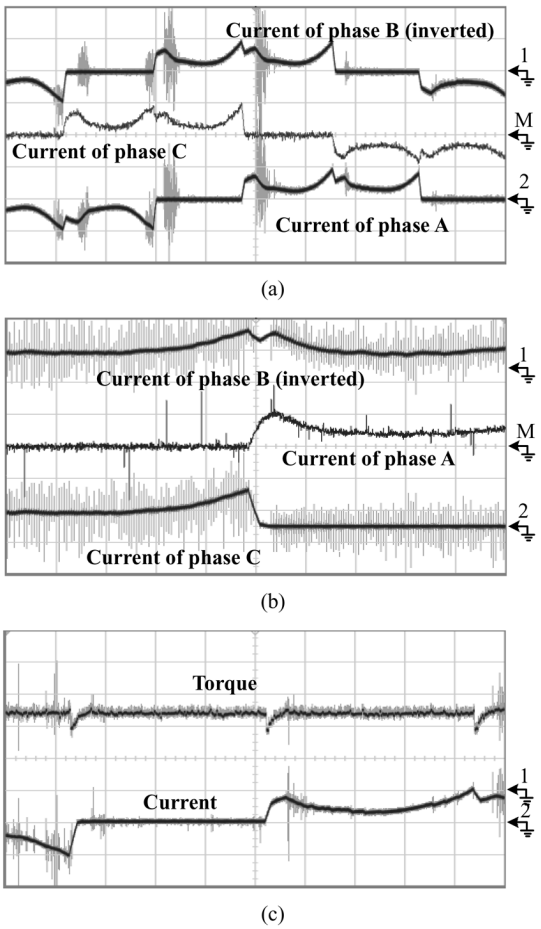

Fig. 14. Torque control neglecting finite dc bus supply voltage. (a) Three phase currents (10 A/div, 5 ms/div). (b) Currents (10 A/div, 1 ms/div) commutation. (c) Torque (2.54 Nm/div) and phase current (10 A/div, 2 ms/div).

C. Experimental Results

Fig. 13 shows the torque and phase current of the brushless dc motor with un-ideal back EMF waveforms with conventional rectangular current control. Torque ripple is obvious in both normal conduction period and commutation period even though the current waveform is close to rectangular.

Fig. 14 shows the experimental results with torque control neglecting finite dc bus supply voltage. In Fig. 14(a), currents become different because the objective is not to control the current rectangular but to make the torque feedback follow the torque reference. Fig. 14(b) shows a detailed commutation process, a current dip produces in the un-commutated phase current because the slope of the outgoing phase current is fast but the slope of the incoming phase current is slow. In Fig. 14(c), torque ripple in the normal conduction period has been reduced, but the commutation torque ripple also exists in commutation period due to finite dc bus supply voltage.

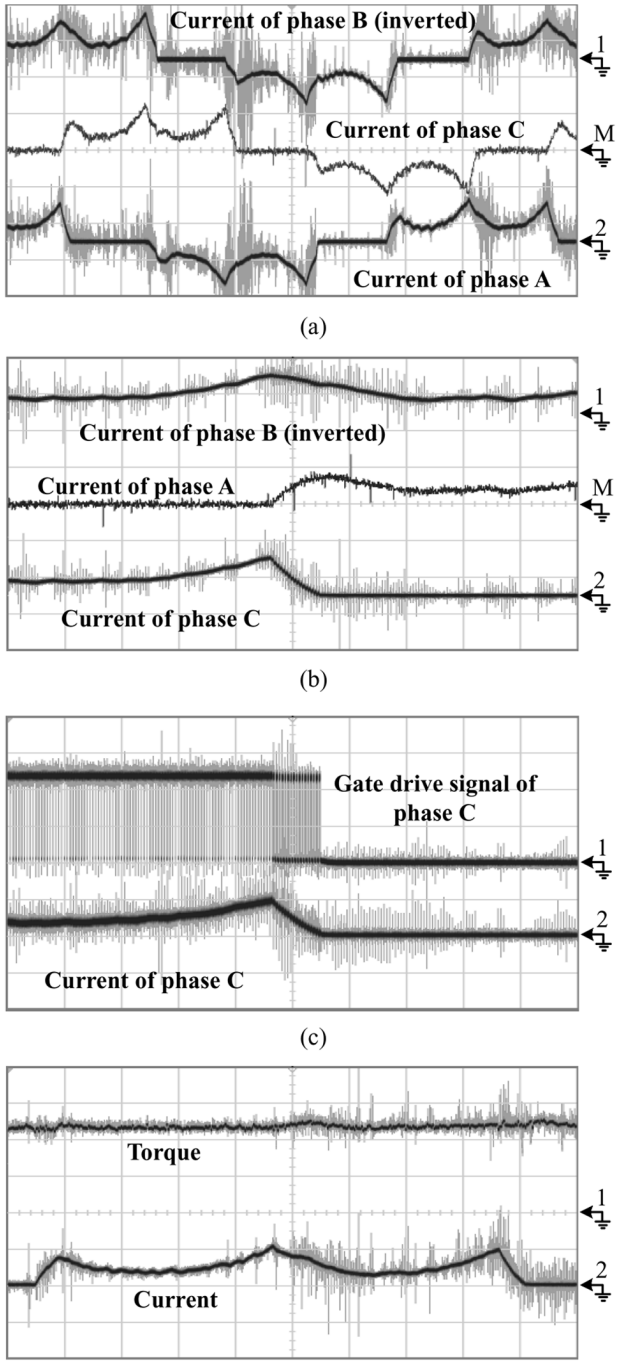

Fig. 15. Torque control considering finite dc bus supply voltage. (a) Three phase currents (10 A/div, 5 ms/div). (b) Currents (10 A/div, 1 ms/div) commutation. (c) Gate drive signal (2 V/div) used to control the outgoing phase current (10 A/div, 1 ms/div). (d) Torque (2.54 Nm/div) and phase current (10 A/div, 2 ms/div).

Fig. 15 shows the experimental results with torque control considering finite dc bus supply voltage. In Fig. 15(a), the current dip in the un-commutated phase current is reduced. Fig. 15(b) describes a detailed commutation process. The slope of the outgoing phase current has been slowed down by controlling the corresponding switch, whose gate drive signal

TABLE I
COMPARISON RESULTS WITH EXISTING METHODS

Method	Required sensors*	Coordinate transformation	Conduction mode	Instantaneous torque observer
3-phase reference current waveform	AC	N	3-phase	N
dq reference current waveform	AC	Y	3-phase	N
Instantaneous torque control	AC+DC	Y	3-phase	Y
Direct torque control	AC+DC	Y	2-phase	Y
Presented method	AC+DC	N	2-phase	N

* AC: phase current sensors. DC: DC-link voltage sensor.

is shown in Fig. 15(c). Fig. 15(d) shows that torque ripples in both the normal conduction period and the commutation period are reduced.

Some results compared with existing methods are shown in Table I. From this table, it can be seen that both coordinate transformation and instantaneous torque observer are not necessary in the presented method.

IV. CONCLUSION

A new torque control method is proposed in this paper to reduce torque ripple of BLDC motors with un-ideal back EMF waveforms.

In this method, duty cycle D_n, D_c, and D_o, which are, respectively, used to control the corresponding switches, are calculated in the torque controller. In the commutation period, the finite dc bus supply voltage and the resulting finite ability of the torque controller are considered. When the un-commutated phase current is distorted, the slope of the outgoing phase current is slowed down to attenuate the current dip produced in the commutation period, as well as the commutation torque ripple. The simulation and experiment results carried out in a 4 kW BLDC motor prototype verify the validity of the proposed torque control method.

APPENDIX
PARAMETERS OF THE BLDC MOTOR

Number of poles 4
Rated power 4 kW
Rated voltage 300 V
Rated speed 3000 r/min
Resistance 0.059 Ω
Inductance 0.29 mH

REFERENCES

[1] P. Pillay and R. Krishnan, "Modeling, simulation, and analysis of permanent-magnet motor drives, part II: The brushless dc motor drive," *IEEE Trans. Ind. Appl.*, vol. IA-25, no. 2, pp. 274–279, Mar./Apr. 1989.

[2] H. Le-Huy, P. Perret, and R. Feuillet, "Minimization of torque ripple in brushless dc motor drives," *IEEE Trans. Ind. Appl.*, vol. IA-22, no. 4, pp. 748–755, Jul./Aug. 1986.

[3] J. Y. Hung and Z. Ding, "Design of currents to reduce torque ripple in brushless permanent magnet motors," in *Proc. IEE*, Jul. 1993, vol. 140, pp. 260–266, no. 4.

[4] E. Favre, L. Cardoletti, and M. Jufer, "Permanent-magnet synchronous motors: A comprehensive approach to cogging torque suppression," *IEEE Trans. Ind. Appl.*, vol. 29, no. 6, pp. 1141–1149, Nov./Dec. 1993.

[5] D. C. Hanselman, "Minimum torque ripple, maximum efficiency excitation of brushless permanent magnet motors," *IEEE Trans. Ind. Appl.*, vol. 41, no. 3, pp. 292–300, Jun. 1994.

[6] S. J. Park, H. W. Park, M. H. Lee, and F. Harashima, "A new approach for minimum-torque-ripple maximum-efficiency control of BLDC motor," *IEEE Trans. Ind. Electron.*, vol. 47, no. 1, pp. 109–114, Feb. 2000.

[7] H. W. Park, S. J. Park, Y. W. Lee, S. I. Hong, and C. U. Kim, "Reference frame approach for torque ripple minimization of bldcm over wide speed range including cogging torque," in *Proc. IEEE ISIE*, 2001, pp. 637–642.

[8] T. S. Low, K. J. Tseng, K. S. Lock, and K. W. Lim, "Instantaneous torque control," in *Proc. IEEE ICEMD*, 1989, pp. 100–105.

[9] T. S. Low, K. J. Tseng, T. H. Lee, K. W. Lim, and K. S. Lock, "Strategy for the instantaneous torque control of permanent-magnet brushless dc drives," *Proc. Inst. Elect. Eng.*, vol. 137, pp. 355–363, Nov. 1990.

[10] T. S. Low, T. H. Lee, K. J. Tseng, and K. S. Lock, "Servo performance of a cldc drive with instantaneous torque control," *IEEE Trans. Ind. Appl.*, vol. 28, no. 2, pp. 455–462, Mar./Apr. 1992.

[11] F. Colamartino, C. Marchand, and A. Razek, "Considerations of non-sinusoidal field distribution in a permanent magnet synchronous motor control," in *Proc. IEE PEVSD*, 1994, pp. 508–513.

[12] S. J. Kang and S. K. Sul, "Direct torque control of brushless dc motor with nonideal trapezoidal back-emf," *IEEE Trans. Power Electron.*, vol. 10, no. 6, pp. 796–802, Nov. 1995.

[13] C. French and P. Acarnley, "Direct torque control of permanent magnet drives," *IEEE Trans. Ind. Appl.*, vol. 32, no. 5, pp. 1080–1088, Sep./Oct. 1996.

[14] Y. Liu, Z. Q. Zhu, and D. Howe, "Direct torque control of brushless dc drives with reduced torque ripple," *IEEE Trans. Ind. Appl.*, vol. 41, no. 2, pp. 599–608, Mar./Apr. 2005.

[15] Y. Liu, Z. Q. Zhu, and D. Howe, "Instantaneous torque estimation in sensorless direct-torque-controlled brushless dc motors," *IEEE Trans. Ind. Appl.*, vol. 42, no. 5, pp. 1275–1283, Sep./Oct. 2006.

[16] R. Carlson, M. L. Mazenc, and J. Fagundes, "Analysis of torque ripple due to phase commutation in brushless DC machines," *IEEE Trans. Ind. Appl.*, vol. 28, no. 3, pp. 632–638, May/Jun. 1992.

[17] C. S. Berendsen, G. Champenois, and A. Bolopion, "Commutation strategies for brushless DC motors: Influence on instant torque," *IEEE Trans. Power Electron.*, vol. 8, no. 2, pp. 231–236, Apr. 1993.

[18] L. Zhang and W. L. Qu, "Commutation torque ripple restraint in BLDC motor over whole speed range," in *Proc. IEEE ICEMS*, 2005, pp. 1501–1507.

[19] J. H. Song and I. Choy, "Commutation torque ripple reduction in brushless dc motor drives using a single dc current sensor," *IEEE Trans. Power Electron.*, vol. 19, no. 2, pp. 312–319, Mar. 2004.

[20] D. K. Kim, K. W. Lee, and B. I. Kwon, "Commutation torque ripple reduction in a position sensorless brushless dc motor drive," *IEEE Trans. Power Electron.*, vol. 21, no. 6, pp. 1762–1768, Nov. 2006.

Haifeng Lu was born in Shangdong, China, in 1976. He received the B.S. and M.S. degrees from Southeast University, Nanjing, China, in 1998 and 2001, respectively, and the Ph.D. degree from the Tsinghua University, Beijing, China, in 2005, all in electrical engineering.

Since 2005, he has been with the Department of Electrical Engineering, Tsinghua University, serving as an Assistant Professor. His current major research interests are in power electronics and motor drives.

Lei Zhang was born in Anhui, China, in 1979. He received the B.S. degree from Xi'an Jiaotong University, Xi'an, China, in 2002, and the Ph.D. degree in electrical engineering from Tsinghua University, Beijing, China, in 2007.

Since 2007, he has been with Santak Electronics, Ltd. Co., Guangdong, China, where he currently is a Staff Member in the Research and Development Center. His research interests are control of permanent magnet motors, power electronics for wind turbines, and DSP techniques.

Wenlong Qu was born in Shanghai, China, on February 6, 1946. He received the Ph.D. degree from the Department of Electrical Engineering, Tsinghua University, Beijing, China, in 1970.

Since 1970, he has been a Teacher in the Department of Electrical Engineering, Tsinghua University where he is currently a Professor. He is the author of more than 70 technical papers in power electronics and motor control. His research interests include ac and dc motor controls, dc–dc converters, soft-switching techniques, electric vehicle drives and power steering system control.